Static Mechanics and Dynamic Analysis and Control of Bridge Structures Under Multi-Load Coupling Effects

Ma Zhifang*, Sun Zhuoyu and Yuan Yuan

Zhengzhou Railway Vocational & Technical College, Zhengzhou Henan 450000, China
E-mail: mazhifang@zzrvtc.edu.cn
**Corresponding Author*

Received 13 September 2023; Accepted 06 October 2023;
Publication 03 November 2023

Abstract

With the rapid development and wide application of large-span bridges, the problem of dynamics and safety control of bridge structures under multiple loads is becoming more and more prominent. To realize the dynamic analysis and mechanical control of the girder structure, this paper designs a new type of magnetorheological (MR) mechanical damper based on the mechanistic analytical method and establishes a coupled dynamics model of the vehicle-rail-MR mechanical damper. The simulation and validation results show that the error between the semi-analytical method and the finite element theory calculation results is only 1.0%, while the kinetic simulation is consistent with the measured frequency domain trend. The analytical results show that: After applying MR mechanical damper for mechanical control, the moment live load and shear values of side spans were reduced by 27.68% and 10.79%, respectively; and the maximum moment and shear values generated at the center pivot were reduced by 28.19% and 10.81%, respectively. After applying the mechanical damper, the stress distribution of the cable-stayed bridge is more balanced, and the maximum diagonal stress of the overall structure

European Journal of Computational Mechanics, Vol. 32_4, 369–392.
doi: 10.13052/ejcm2642-2085.3243

is reduced from 3.8 MPa to 2.9 MPa. After safety control, the root-mean-square (RMS) value of the mid-span displacement amplitude was reduced by 59.32% and the maximum value was reduced by 11.46%, which improved the stability of the girder dynamics. After mechanical control, the dynamic acceleration response of the beam within the span decreased between 2 and 8 seconds and increased between 8 and 10 seconds. The overall response fluctuated around -5 m/s^2 with a relatively smooth trend.

Keywords: Static mechanics, dynamics, bridge structures, multi-loading, MR mechanics damper, mechanical control.

1 Introduction

In recent years, with the widespread rise and rapid development of large-span bridge construction, the construction environment of bridge structures has become more and more complex, as shown in Figure 1. Among them, the safety of bridge vibration under multiple loads has also increased. The safety of bridge use concerns the safety of people and vehicles, and to ensure the safety and stability of people, vehicles, and bridges, it is necessary to reduce the vibration response of the bridge structure, which is usually carried out using structural vibration Mechanical control. The working principle of structural vibration Mechanical control is that it requires two parts to operate together, namely the Mechanical control system and the structure, which together can effectively resist external power inputs, and is considered to be a proactive measure to reduce the dynamic response of the structure".

Figure 1 Structural engineering schematic of various types of suspension and cable-stayed bridges.

Therefore, vibration Mechanical control of bridge structures has attracted strong attention from many scholars not only in academia but also in the engineering community, and important developments have been made [2]. However, since the geometry, construction form, dynamic properties, and operating conditions of bridge structures are very different from those of housing structures and towering structures, the study of vibration Mechanical control of bridge structures has its specificity in the fields of theoretical foundation, device design, and engineering practice. Structural vibration Mechanical control under multiple loads is an engineering problem with a wide range of applications, which refers to the use of measures to safely control the response of structures under multiple sources of dynamic loads to meet engineering requirements, and the related research was first initiated in mechanical engineering in the twentieth century, and then developed to aerospace and transportation engineering and civil engineering. As one of the world's seven major hazards, environmental vibration to the bridge structure has brought indelible impact, Taking effective vibration reduction measures to eliminate its adverse effects is the current research hotspot. Bridges will vibrate, mainly due to the role of external excitation such as earthquakes, wind, vehicles, water waves, etc. However, with the increase in the number of vehicles, loads, and speeds, the vibration of bridges will be enhanced, and the bridges will be damaged. The principle of vibration Mechanical control is mainly used to reduce the vibration of bridge structures, due to its many advantages such as simplicity and convenience, economic practicality, and better safety. In recent years, theoretical and experimental research on structural vibration Mechanical control has developed rapidly, which also promotes the rapid development of structural vibration Mechanical control technology in practical engineering. The classification principle of bridge structural vibration Mechanical control can be categorized as passive Mechanical control, active Mechanical control, semi-active Mechanical control, and hybrid Mechanical control problems if it adopts whether or not additional energy is required.

In terms of active Mechanical control, Truong et al. investigated the aeroelastic active Mechanical control of a suspension bridge using both experimental and numerical methods [4]. DH Phan's method of active Mechanical control using a Mechanical control surface system with airfoils helped the long suspension bridge to reach a steady state of flutter and shivering vibration [5]. Lasangalli et al. proposed a flow-structure coupled scheme for active Mechanical control of bridge flutter instability numerical simulation with a fluid-structure coupling scheme, which suppresses

or attenuates the dynamic instability induced by wind action on large-span bridges [6]. KK Bera et al. investigated active Mechanical control of large-span cable-stayed bridges for flutter vibration by using a winglet driven by a constant/variable-gain output-feedback Mechanical controller [7]. RW Soares et al. devised a practically implementable implementation-based adaptive Mechanical control method for the seismic response of bridges, which can effectively reduce the seismic response and maintain the overall performance of the system well [8]. C. Mei proposed a hybrid method for active Mechanical control of beam bending vibration based on advanced Timoshenko theory, applying fluctuating Mechanical control at one or more points in the structure, and applying fluctuating Mechanical control at one or more points in the structure [9].

In the area of passive Mechanical control, HJ Jung et al. conducted a study of an intelligent passive system with magnetorheological dampers for benchmark highway bridge models under different historical earthquakes, and the implementation of this intelligent passive Mechanical control system verified the effectiveness of seismic protection for the benchmark problem of seismically-excited highway bridges [10], and Rosario Ceravolo et al. focused on the installation of a passive vibration Mechanical control system for dynamic identification strategies of complex bridge structures [11], Martinez-Rodrigo et al. proposed and evaluated the possibility of retrofitting the original bridge with various passive additional damping and seismic isolation systems to improve the structural response in the vertical direction [12], and Soneji et al. investigated the seismic performance of passive hybrid Mechanical control systems for cable-stayed bridges under actual ground shaking conditions, and the results showed that the seismic performance of The addition of additional damping in the form of viscous fluid dampers significantly reduces the seismic response of isolated cable-stayed bridges [13], Wilde et al. proposed a passive pneumatic Mechanical control method for bridge flutter. The system consists of two additional surfaces to generate stabilizing forces [14].

a. In terms of semi-active Mechanical control, Soto et al. investigated that combining traditional passive Mechanical control (base isolation) with a semi-active system resulted in significant vibration damping compared to traditional passive Mechanical control [15], SJ et al. installed a hybrid Mechanical control system consisting of a semi-active magnetorheological (MR) damper and passive base isolation bearings on bridge decks and piers for vibration damping of highway bridge structures,

and GHeo et al. investigated a hybrid Mechanical control algorithm of a semi-active Mechanical control device to effectively and safely control the drift induced by earthquake loads on a multi-span bridge superstructure [16] where the MR damper (also known as base isolation) was used. studied a hybrid Mechanical control algorithm for a semi-active Mechanical control device to effectively and safely control the drift induced by seismic loads on seismically isolated multi-span bridge superstructures [16]. Among them, the MR damper (also known as magnetorheological damper) can be used as a high-performance variable damping device for semi-active Mechanical control of civil engineering structures by its several excellent characteristics, such as low energy consumption, simple structure, high output power, and high controllability. The MR damper can quickly adjust the damping force by adjusting the voltage and current according to the real-time response of the structure, such as displacement response and velocity response, so it has intelligent damping characteristics and vibration Mechanical control effect close to the active Mechanical control, and the power consumption is lower compared with the active Mechanical control. MR damper can only provide the force opposite to the direction of motion, which is due to it providing Mechanical control force in the form of damping force, and Mechanical control force in the form of damping force. This is because the Mechanical control force is provided in the form of a damping force, and the direction of the Mechanical control force is limited. However, because of this, the MR damper has a stable working performance and very good robustness. It is easy to find that MR dampers are very suitable for the vibration Mechanical control of civil engineering structures. Safety issues such as static mechanics and dynamics of bridges have received the attention of many scholars and engineers, and certain research results have been achieved [17–22]. But the majority of existing seismic design codes for bridge engineering at home and abroad, it is still only applicable to medium-span bridges, and there is no way to do anything for large-span bridges exceeding the scope of application. Scholars from various countries have conducted much research on the seismic design of large-span arch bridges, and many scholars such as Fan Lizhu, Hu Shide, Ye Aijun, and Li Jianzhong in China have conducted a lot of research on this and achieved some results in the seismic design of large-span bridges, but at present, there is no unified standard for the seismic design of large-span arch bridges, and there are fewer researches on the application of MR dampers on arch

bridges. Smart materials have made a lot of contributions to the research and application of vibration Mechanical control of bridges in recent years [23–27], MR damper can be used as its representative by several excellent characteristics, and considering a variety of vibration Mechanical control modes found that the integrated performance of semiactive Mechanical control is excellent, and the combination of MR damper and semiactive Mechanical control and its application to the vibration Mechanical control of bridge structures has a broad application prospect. Conventional dampers mainly dissipate energy through friction, viscous damping, and material damping. These damping mechanisms mainly achieve the purpose of energy dissipation by converting mechanical energy into thermal energy. MR mechanical dampers, on the other hand, are based on the characteristics of magnetorheological fluids, and the viscosity of magnetorheological fluids is changed by changing the magnetic field strength, to control the damping characteristics of the damper. Therefore, based on the combination of the semi-analytical method and finite element method [28–30], a new MR damper is optimally designed based on mechanical theory. At the same time, the coupled model of axle-MR damper under multiple loads is established to calculate the dynamic behavior before and after Mechanical control and Mechanical control study. Eventually, MR Mechanical Dampers can enhance the stability of bridge structures and reduce the vibration acceleration of girders under multiple loads.

2 Bridge Mechanical Modeling Analysis

Arch The research object of this paper is a bridge over the Jinsha River, which is a cable-stayed bridge and an important river crossing bridge across a place in Yunnan and Sichuan. The bridge is 507.825 m long, spanning up to 188 m, arch axis coefficient m = 2.099, vector span ratio of 1/4, approach arrangement: 7 × 25m prestressed concrete hollow slab bridge, Yunnan bank approach bridge is 183m long; Sichuan bank approach bridge arrangement: 5 × 25 m prestressed concrete hollow slab bridge, Sichuan bank approach bridge is 128.025 m long. the bridge deck for the average of 3 cm – seismic intensity 7 degrees. The seismic intensity is 7 degrees. The intrinsic frequency and modal vibration pattern of the structure are its intrinsic characteristics, which are only related to its own mass, stiffness distribution, and material properties, and have nothing to do with the external conditions. In the dynamic analysis, the intrinsic characteristics such as the

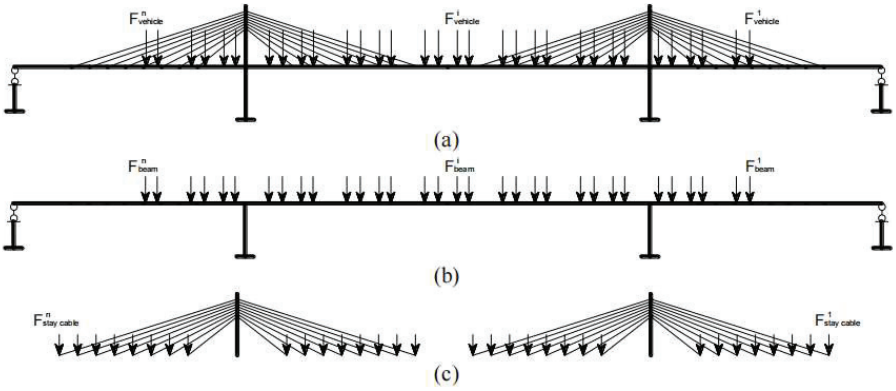

Figure 2 Mechanical action of bridge structures.

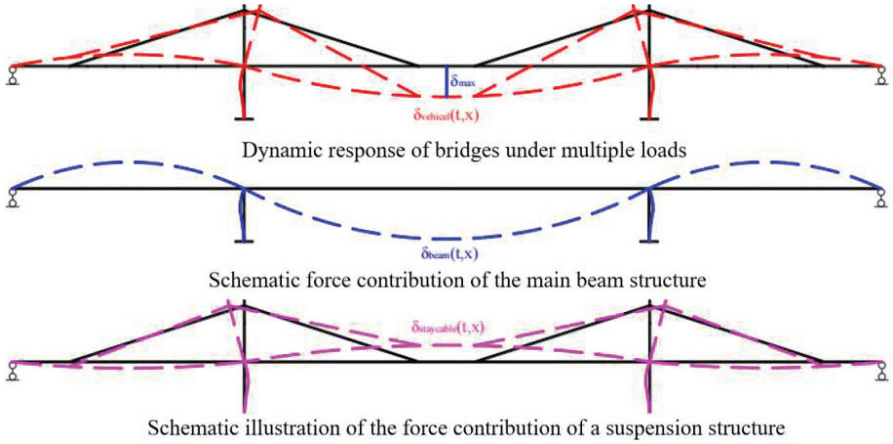

Figure 3 Schematic distribution of forces contributed by the bridge.

self-oscillation frequency of the structure can be understood through modal analysis. In structural dynamics, it is generally believed that the contribution of low-order modes to the structural response is larger, while the contribution of higher-order modes is smaller, therefore, for complex structures, we only need to retain the low-order modes and use the semi-analytical method in the form of linear superposition to solve the mechanical properties of the structure. In this case, the schematic diagram of the bridge subjected to load is shown in Figure 2. The schematic diagram of the shared load contributed by different members is shown in Figure 3.

Since the shear center of the beam section does not coincide with the center of mass, taking the shear center of the beam as the coordinate origin and considering the beam vertical, transverse, bending, and torsion coupling as well as the longitudinal deformation, the theoretically resolved fluctuation equations of the beam under the joint action of wind load and temperature force can be written as follows:

$$k_{\mathrm{j}}A_{\mathrm{r}}G\left(\frac{\partial^2 u_y}{\partial x^2}-\frac{\partial\theta_z}{\partial x}\right)-P\left(\frac{\partial^2 u_y}{\partial x^2}-z_0\frac{\partial^2\psi}{\partial x^2}\right)$$
$$-\rho A_{\mathrm{r}}\left(\frac{\partial^2 u_y}{\partial t^2}-z_0\frac{\partial^2\psi}{\partial t^2}\right)=0 \tag{1}$$

$$k_{\mathrm{j}}GA_{\mathrm{r}}\left(\frac{\partial^2 u_z}{\partial x^2}-\frac{\partial\theta_y}{\partial x}\right)-P\left(\frac{\partial^2 u_z}{\partial x^2}-y_0\frac{\partial^2\psi}{\partial x^2}\right)$$
$$-\rho A_{\mathrm{r}}\left(\frac{\partial^2 u_z}{\partial t^2}-y_0\frac{\partial^2\psi}{\partial t^2}\right)=0 \tag{2}$$

$$GJ\frac{\partial^2\psi}{\partial x^2}-I_\alpha\frac{\partial^2\psi}{\partial t^2}-P\left(I_z\frac{\partial^2\psi}{\partial x^2}-z_0\frac{\partial^2 u_y}{\partial x^2}\right)-\rho A_{\mathrm{r}}z_0\frac{\partial^2 u_y}{\partial t^2}=0 \tag{3}$$

$$EA_{\mathrm{r}}\frac{\partial^2 u_x}{\partial x^2}-\rho A_{\mathrm{r}}\frac{\partial^2 u_x}{\partial t^2}=0 \tag{4}$$

$$EI_y\frac{\partial^2\theta_y}{\partial x^2}+k_{\mathrm{j}}A_{\mathrm{r}}G\left(\frac{\partial u_z}{\partial x}-\theta_y\right)-\rho I_y\frac{\partial^2\theta_y}{\partial t^2}=0 \tag{5}$$

$$EI_z\frac{\partial^2\theta_z}{\partial x^2}+k_{\mathrm{j}}A_{\mathrm{r}}G\left(\frac{\partial u_y}{\partial x}-\theta_y\right)-\rho I_z\frac{\partial^2\theta_z}{\partial t^2}=0 \tag{6}$$

Where: u_y is the transverse displacement of the beam; θ_z is the transverse bending angle; ψ is the torsion angle of the beam; u_z is the vertical displacement of the beam; θ_y is the vertical bending angle; u_x is the axial displacement of the beam; P is the axial force of the beam, which is positive in compression; z0 is the distance from the center of the section to the center of the shear center; E is Young's modulus of the beam; ρ is the density of the beam; Ar is the area of the beam; k_{j} is the shear factor; G is the shear stiffness; Iz and Iy are the moments of inertia of the beam about the z- and y-axes, respectively; is the rotational inertia of the beam. Iz and Iy are the moments of inertia of the beam around the z-axis and y-axis, respectively; I_α is the moment of inertia of the beam.

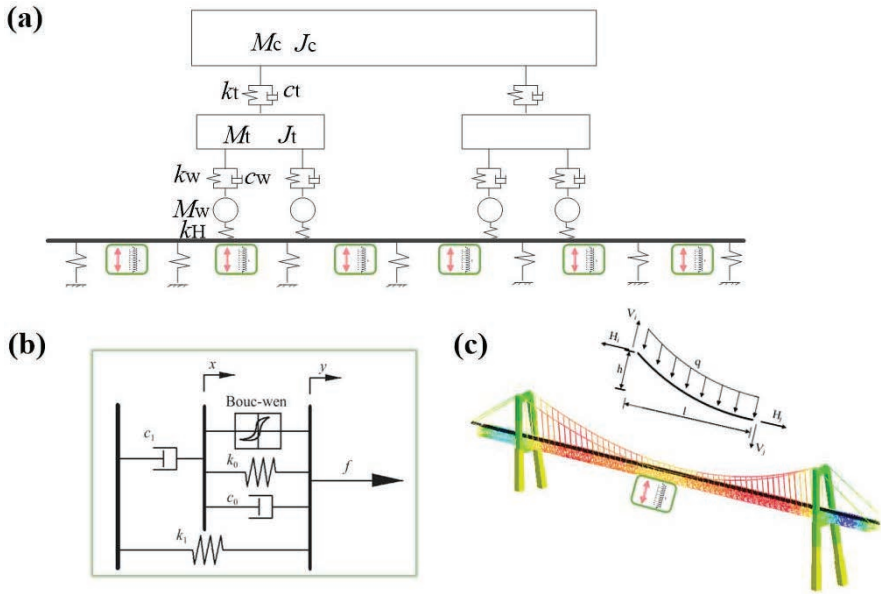

Figure 4 Coupling mechanics modeling and MR damper mechanics modeling.

The semi-analytical model of axle coupling dynamics and the mechanical model of the MR damper are shown in Figure 4. The mechanical equation of the MR damper is given by

$$F_{\mathrm{MR}} = f_0 \,\mathrm{sgn}(\dot{x}) + c\dot{x} + kx \tag{7}$$

Where, F – the output damping force of the MR damper; *for* – the initial friction force; *sgn*(x) – the sign function to change the direction of the Mechanical control force; c – the viscous damping coefficient of the damper; x – the magnitude of the velocity of the damper piston rod; k – the stiffness coefficient of the spring unit.

To analyze the dynamic response of the track structure under the action of mobile vehicle loads, the vehicle system is considered as a 10-degree-of-freedom multi-rigid body model, as shown in Figure 5-18, and the vibration equation of the vehicle system can be established by adopting Hamilton's principle, which can be used to obtain the mass, stiffness, and damping matrix. The mass matrix of the vehicle system can be expressed as:

$$\mathbf{M}_{\mathrm{v}} = \mathrm{diag}[M_{\mathrm{c}}, J_{\mathrm{c}}, M_{\mathrm{t}}, J_{\mathrm{t}}, M_{\mathrm{t}}, J_{\mathrm{t}}, M_w, M_w, M_w, M_w] \tag{8}$$

The vehicle system stiffness matrix and damping matrix are:

$$\mathbf{K}_{\mathrm{v}}=\begin{bmatrix}
2k_{\mathrm{t}} & 0 & -k_{\mathrm{t}} & -k_{\mathrm{t}} & 0 & 0 & 0 & 0 & 0 & 0\\
 & 2b^2k_{\mathrm{t}} & -bk_{\mathrm{t}} & -bk_{\mathrm{t}} & 0 & 0 & 0 & 0 & 0 & 0\\
 & & 2k_{\mathrm{w}}+k_{\mathrm{t}} & 0 & 0 & 0 & -k_{\mathrm{w}} & -k_{\mathrm{w}} & 0 & 0\\
 & & & 2k_{\mathrm{w}}+k_{\mathrm{t}} & 0 & 0 & 0 & 0 & -k_{\mathrm{w}} & -k_{\mathrm{w}}\\
 & & & & 2a^2k_{\mathrm{w}} & 0 & -ak_{\mathrm{w}} & ak_{\mathrm{w}} & 0 & 0\\
 & & & & & 2a^2k_{\mathrm{w}} & 0 & 0 & -ak_{\mathrm{w}} & ak_{\mathrm{w}}\\
 & & & & & & k_{\mathrm{w}} & 0 & 0 & 0\\
 & & & \text{symmetry} & & & & k_{\mathrm{w}} & 0 & 0\\
 & & & & & & & & k_{\mathrm{w}} & 0\\
 & & & & & & & & & k_{\mathrm{w}}
\end{bmatrix} \tag{9}$$

$$\mathbf{C}_{\mathrm{v}}=\begin{bmatrix}
2c_{\mathrm{t}} & 0 & -c_{\mathrm{t}} & -c_{\mathrm{t}} & 0 & 0 & 0 & 0 & 0 & 0\\
 & 2b^2c_{\mathrm{t}} & -bc_{\mathrm{t}} & -bc_{\mathrm{t}} & 0 & 0 & 0 & 0 & 0 & 0\\
 & & 2c_{\mathrm{w}}+c_{\mathrm{t}} & 0 & 0 & 0 & -c_{\mathrm{w}} & -c_{\mathrm{w}} & 0 & 0\\
 & & & 2c_{\mathrm{w}}+c_{\mathrm{t}} & 0 & 0 & 0 & 0 & -c_{\mathrm{w}} & -c_{\mathrm{w}}\\
 & & & & 2a^2c_{\mathrm{w}} & 0 & -ac_{\mathrm{w}} & ac_{\mathrm{w}} & 0 & 0\\
 & & & & & 2a^2c_{\mathrm{w}} & 0 & 0 & -ac_{\mathrm{w}} & ac_{\mathrm{w}}\\
 & & & & & & c_{\mathrm{w}} & 0 & 0 & 0\\
 & & & \text{symmetry} & & & & c_{\mathrm{w}} & 0 & 0\\
 & & & & & & & & c_{\mathrm{w}} & 0\\
 & & & & & & & & & c_{\mathrm{w}}
\end{bmatrix} \tag{10}$$

The subscripts c, t, and w are the vehicle body, bogie, and wheelset. The meanings of the variables are as follows, M_{c} J_{c} for the mass and moment of inertia of the vehicle body; $M_{\mathrm{t}}, J_{\mathrm{t}}$ for the mass and moment of inertia of the bogie; M_{w} for the mass of the wheelset; k_{w} k_{t} for the suspension stiffness of the vehicle's first and second systems; c_{w} c_{t} for the suspension damping of the vehicle's first and second systems; a is half of the fixed axle spacing of the bogie; and b is half of the fixed spacing of the vehicle. The relevant parameters were finalized mainly through available data and literature [27–30].

The matrix solution form is formed by combining all the above equations:

$$\tilde{\mathbf{D}}\tilde{\mathbf{U}}=\tilde{\mathbf{P}} \tag{11}$$

In terms of the modal validation of the model, the validation results of the semi-analytical method and the finite element theory are shown in Figure 5, and the error values are less are within 1.0%. However, the efficiency of the semi-analytical joint method can be significantly improved.

In addition, to further verify the correctness of the train dynamics model establishment, this paper selects a line of measured unevenness as an external

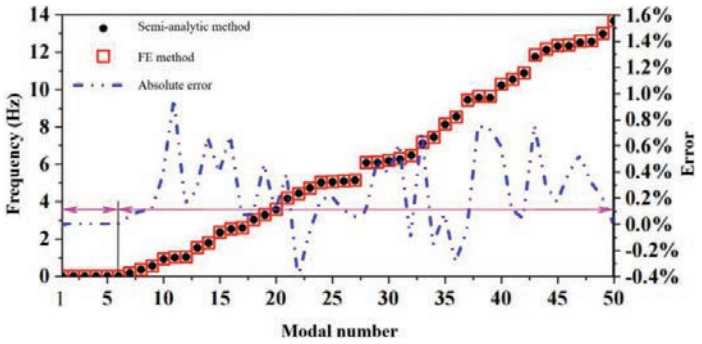

Figure 5 Modal validation of mechanical models.

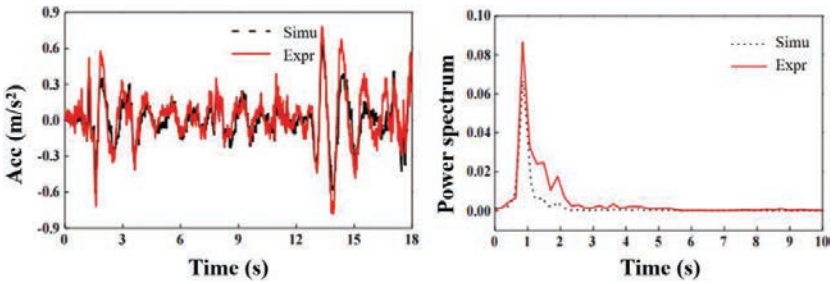

Figure 6 Validation of axle dynamics calculations.

excitation, and adopts the line of measured car body vertical acceleration time domain and frequency domain data comparison to verify, as shown in Figure 6. It can be seen from the figure that the simulation and the measured frequency domain trend are consistent, and the most value is close to it, at the same time, it can be seen from the analysis of the power spectral density of the vehicle's main frequency is consistent, so that the model establishment of the vehicle is Therefore, the vehicle model is accurate and can be used for subsequent research.

3 Statics and Dynamics Utility Before and After Mechanical Control

This paper relies on the improved Bingham model, makes appropriate modifications and simplifications, and optimizes the design to be suitable for this paper to use the basic mechanical model of the MR damper. In this section, the internal force changes in the key parts of the bridge when the vehicle

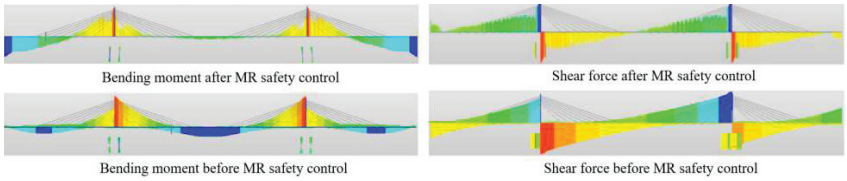

Figure 7 Comparison of bending moment and shear force of the bridge before and after the application of mr mechanical dampers.

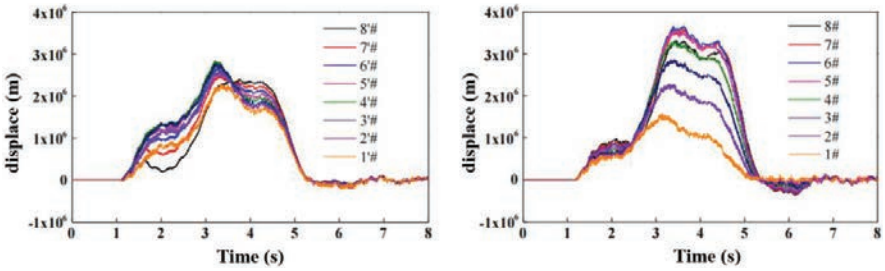

Figure 8 Comparison of stress distribution of each tension cable of the bridge body.

passes through are investigated, and a short tower cable-stayed bridge with a design speed of 350 km/h, a span of (103 + 180 + 103) m, and a pier-beam-tower using the cementation method is selected for the vehicle-bridge coupling calculations, and the changes in the internal forces in the key parts are obtained from Equation (2.37). Firstly, the toy and shear force diagrams before and after the addition of MR mechanical dampers are extracted. It is shown in Figure 7. It can be seen that after the application of the MR mechanical damper, the values of the moment live load and shear force in the side span are 27.68% and 10.79% respectively. After applying the MR mechanical damper, the maximum bending moment and shear force values at the center pivot point are 28.19% and 10.81% of the values before application, respectively. In summary, the mechanical damper can effectively relieve the most unfavorable moment stress and shear stress values of the bridge structure itself.

In addition, the stresses distributed among the tension cables of the cable-stayed bridge after the application of the mechanical damper are more balanced, and the maximum tension stress of the structure as a whole is reduced from 3.8 MPa to 2.9 MPa, and the results are shown in Figure 8.

Before carrying out the dynamic simulation, it is considered that the beam model will first be subjected to its gravity, at which time there is no

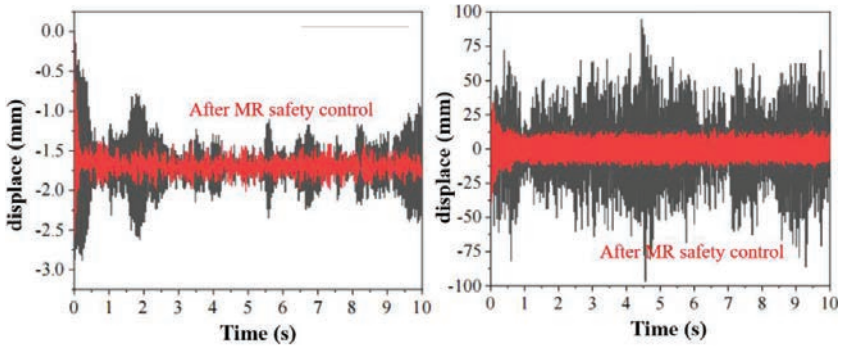

Figure 9 Comparison of beam dynamic displacement response.

Table 1 The price effect of each performance before and after MR Mechanical control (rms/amplitude)

Performance Indicators	Pre-control	Post-control	Effect	Pre-control	Post-control	Effect
Mid-span displacement	0.3	0.12	59.32%	2.88	2.55	11.46%
Mid-span acceleration	28.28	5.68	79.91%	94.62	34.21	63.85%

external force change. Inputting the external excitation of 0∼40 Hz random train signal to the model beam, the mid-span displacement response time-domain curves and the mid-span acceleration response time-domain curves before and after applying the Mechanical control of MR mechanical damper can be obtained as shown in Figure 9. From the beam mid-span displacement time-domain curve and the beam mid-span acceleration time-domain curve, it can be observed that the time needed for the beam to converge to the steady state after applying the active Mechanical control is reduced, and the hydraulic adaptive active Mechanical control support is beneficial to reduce the vibration of the beam and improve the stability of vibration, which is conducive to the safe, fast and smooth passage of the vehicle. Analyzing the time-domain curves of mid-span displacement and acceleration before and after the model Mechanical control under random excitation, Table 1 is obtained. In the case of the model, A condition subject to external excitation, the root-mean-square (RMS) value of mid-span displacement amplitude is reduced by 59.32% and the maximum value of the amplitude is reduced by 11.46%; the RMS value of mid-span acceleration amplitude is reduced by

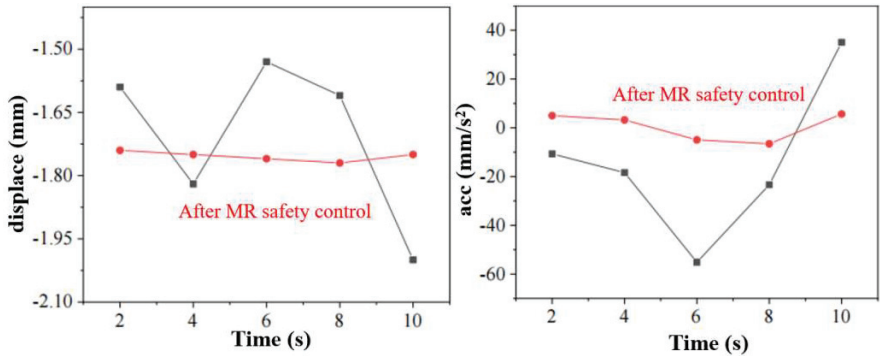

Figure 10 Comparison of moment diagrams of displacement response before and after mechanical control.

79.91% and the maximum value of the amplitude is reduced by 63.85% after the Mechanical control – 63.85%. The reduction of the root mean square value of the amplitude shows the effectiveness of the adaptive bearing Mechanical control and improves the stability of the beam vibration; the removal of the maximum value of the amplitude proves that the extreme response of the beam vibration is reduced, and reduces the possibility of structural damage of the beam due to the amplitude is too large, which all contribute to the safe, fast and smooth passage of the vehicle.

As shown in Figure 10, The moment diagrams of mid-span displacement and mid-span acceleration response of the bridge model under the random excitation of the train are given. From Figure 10, it can be seen that the response of mid-span displacement before Mechanical control decreases from 2 s to 4 s, increases from 4 s to 6 s, decreases from 6 s to 8 s, and decreases from 8 s to 10 s, and the curve fluctuates greatly, with the overall change between −1.57 mm and −2.05 mm; the response of mid-span displacement after Mechanical control decreases from 2 s to 4 s decreases from 4 s to 6 s, decreases from 6 s to 8 s, and increases from 8 s to 10 s, with the overall change between −1.57 mm and −2.05 mm. After Mechanical control, the mid-span displacement response decreases from 2 s to 4 s, decreases from 4 s to 6 s, decreases from 6 s to 8 s, and increases from 8 s to 10 s, with the overall response fluctuating around −1.72 mm and the trend of change is relatively smooth. It can be seen that the response of the mid-span acceleration before Mechanical control decreases from 2 s to 4 s, the response decreases from 4 s to 6 s, the response increases from 6 s to 8 s, and the response increases from 8 s to 10 s, and the curve fluctuates greatly,

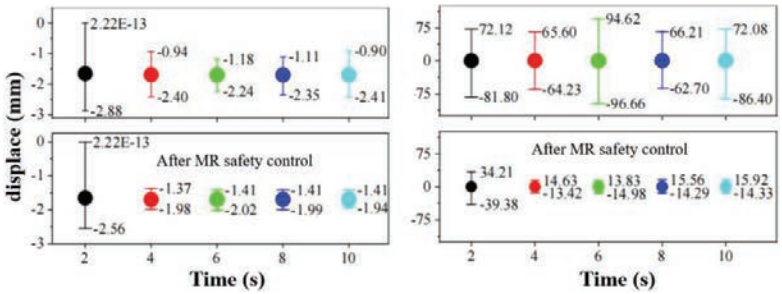

Figure 11 Comparison of ultimate displacement before and after mechanical control.

and the overall response fluctuates from -58 m/s^2 to -40 m/s^2; the response of the mid-span acceleration after Mechanical control decreases from 2 s to 4 s, the response decreases from 4 s to 6 s, the response decreases from 6 s to 8 s, and the overall response fluctuates from -1.72 mm, and the trend of change is relatively smooth. After the Mechanical control, the mid-span acceleration response decreases from 2 s to 4 s, decreases from 4 s to 6 s, increases from 8 s to 10 s, and fluctuates from -5 m/s^2 to -40 m/s^2, which is a relatively smooth change trend. It can be concluded that the vibration of the bridge is smoother and the vibration response of the bridge is reduced after the implementation of Mechanical control.

Interval plots of displacement and acceleration changes in the span before and after the Mechanical control at intervals of 2 s, as shown in Figure 11, indicate the magnitude of the extreme deviation. The extreme difference value is the difference between the largest and the smallest data in a set of data, which is often used to express the degree of dispersion of a set of data. It can be seen that the fluctuation range of span-to-span displacement before Mechanical control is -2.88 mm$\sim$zero point in 0$\sim$2 s, and the fluctuation range of 8 s$\sim$10 s is -2.41 mm~-0.90 mm, and the overall fluctuation range is -2.88 mm$\sim$zero point; the fluctuation range of span-to-span displacement after Mechanical control is -2.56 mm$\sim$zero point in 0$\sim$2 s, and the fluctuation range of 8 s$\sim$10 s is -1 mm$\sim$0.90 mm, and the overall fluctuation range is -1.88 mm$\sim$zero point. After continuous simulation, the fluctuation range of mid-span displacement in 0$\sim$2 s after Mechanical control is -2.56 mm$\sim$zero point, and after continuous simulation, the fluctuation range in 8 s$\sim$10 s is -1.94 mm~-1.41 mm, and the overall fluctuation range is -2.56 mm$\sim$zero point. The fluctuation range of mid-span acceleration is -81.80 m/s$^2\sim$72.12 m/s^2 in 0–2 s before Mechanical control, and the fluctuation range is -86.40 m/s^2 $\sim$72.08 m/s^2

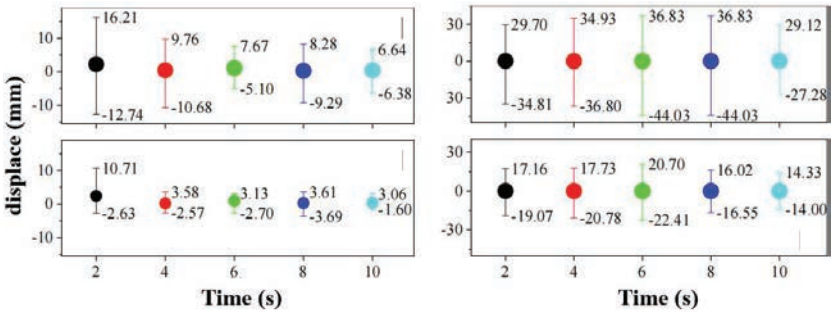

Figure 12 Comparison of end shift before and after mechanical control.

in 8 s∼10 s after successive simulations, and the overall fluctuation range is −96.66 m/s^2∼94.62 m/s^2; the fluctuation range of mid-span acceleration is −39.38 m/s^2∼0.00 m after Mechanical control, and the overall fluctuation range is −39.38 m/s^2∼0.00 m. After Mechanical control, the fluctuation range is smaller than that before Mechanical control. the range is −39.38 m/s^2∼34.21 m/s^2, and after continuous simulation, the fluctuation range of 8 s∼10 s is −14.33 m/s^2∼15.92 m/s^2, and the overall fluctuation range is −39.38 m/s^2−34.21 m/s^2; the fluctuation range becomes smaller than that of the pre-Mechanical control after the Mechanical control, and the extreme deviation value decreases, and the beam's vibration response decreases.

Similarly, as shown in Figure 12, the interval plots of the end part shift of the beam model under random excitation and the change of end acceleration before and after the Mechanical control are shown for every interval of 2 s. The interval plots of the end part shift of the beam model before and after the Mechanical control are shown. it can be seen that the fluctuation range of the safety-controlled front-end part shift is −12.74 mm∼16.21 mm in 0∼2 s, and the fluctuation range of 8 s∼10 s is −6.38 mm∼−6.64 mm after successive simulations, and the overall fluctuation range is between −12.74 mm∼16.21 mm; the fluctuation range of the safety-controlled rear-end part shift in 0–2 s is −2.63 mm∼10.71 mm, after continuous simulation, the fluctuation range of 8 s∼10 s is −1.60 mm∼3.06 mm, and the overall fluctuation range is −2.63 mm∼10.71 mm, the extreme difference value decreases, and the fluctuation range becomes smaller. The fluctuation range of end acceleration in 0–2 s before Mechanical control is −34.81 m/s^2−29.70 m/s^2, and the fluctuation range in 8 s–10 s after continuous simulation is −27.28 m/s^2−29.12 m/s^2, and the overall fluctuation range

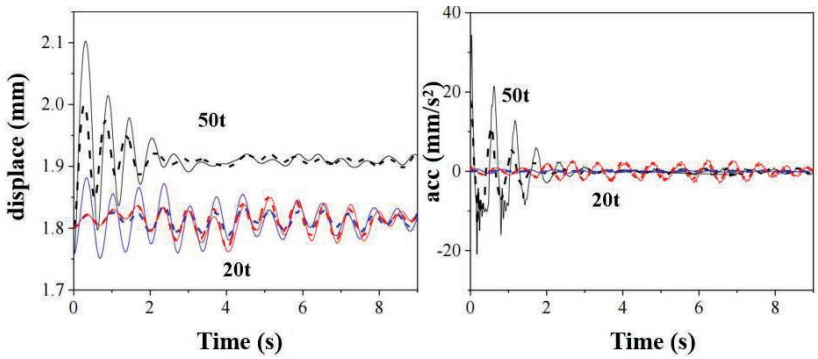

Figure 13 Bridge dynamics effects before and after mechanical control.

is -44.03 m/s^2 -36.83 m/s^2; the fluctuation range of end acceleration in 0–2 s after Mechanical control is -19.07 m/s^2, and the overall fluctuation range is -10.71 mm, and the extreme difference value decreases, and the fluctuation range becomes smaller is -19.07 m/s^2 -17.16 m/s^2, and after continuous simulation, the fluctuation range of 8 s$\sim$10 s is -14.00 m/s^2 -14.33 m/s^2, and the overall fluctuation range is -22.41 m/s^2 -22.70 m/s^2. The fluctuation ranges of the end acceleration after Mechanical control is smaller than those before Mechanical control, the extreme deviation value decreases, and the vibration response of the beams is reduced.

When the bridge deck pavement layer deflection, the change rule is the same. As shown in Figure 13. (where the dotted line represents the control after, the solid line represents the control before) vehicles were traveling to 3.5 s, 4.5 s, and 6 s, the deflection of each span reached the maximum, to the bridge deck pavement layer after the application of MR Mechanical control bridge pavement deflection in each span of the magnitude of the deflection decreased, weakened to the bridge to impose the external excitation brought about by the response. From Figure 13. it can be obtained that due to the decrease in the amplitude of deflection change after the bridge is subjected to Mechanical control, the vibration of the vehicle also changes, the position of the vehicle center of mass droop and acceleration change have been cut down, due to the difference in the weight of a single vehicle 20 t vehicle center of mass droop position, acceleration fluctuation is the largest, the weight of a double vehicle respectively 50 t vehicle center of mass droop position, acceleration fluctuation is the smallest.

Figure 14 can be obtained, due to the bridge by the security control after the deflection change amplitude is reduced, the vehicle vibration also

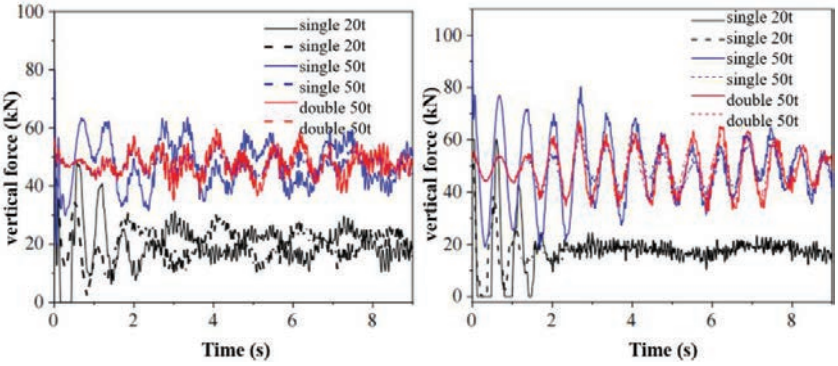

Figure 14 Wheel-track force effects before and after mechanical control.

changed, and the front, center, and rear wheel track force have been cut. The connection between the front axle and the vehicle body is different from that of the middle and rear axles, and the change rule of the middle and rear wheel curves is similar, and the positions of the three wheels overlap with the change curves before and after the vehicle is driven out of the bridge Mechanical control. It shows that after applying the bridge MR Mechanical control, the vibration of the vehicle-axle coupling system such as the beam body and wheel-rail force are significantly attenuated, which can effectively improve the stability of the bridge vibration and the safety of vehicle traveling.

4 Conclusion

(1) After applying the MR mechanical damper for mechanical control, the girder structure was able to effectively mitigate the most unfavorable moment stress and shear stress values of the bridge structure itself. The moment live load and shear stress values at the center span of the side spans are 27.68% and 10.79%, respectively. After the application of the MR mechanical damper, the maximum bending moment and shear stress values generated at the center pivot point are 28.19% and 10.81% of the values before application.

(2) The stress distribution of each tie of the cable-stayed bridge is more balanced, and the maximum tie stress of the structure as a whole is reduced from 3.8 MPa to 2.9 MPa after applying the mechanical damper,

(3) After the mechanical control, the amplitudes of the midspan displacements and accelerations were reduced. Specifically, the root-mean-square (RMS) value of the displacement magnitude was reduced by

59.32% and the maximum value by 11.46%, which demonstrated the effectiveness of the mechanical control of the adaptive bearing and improved the stability of the beam vibration. In addition, the root mean square value of the acceleration amplitude has been reduced by 79.91% and the maximum value has been reduced by 63.85%, which proves that the extreme response of the beam vibration has been reduced, which reduces the possibility of structural damage to the beam due to excessive amplitude. All these changes are in favor of safe, fast, and smooth passage of vehicles.

(4) The mid-span acceleration response decreases from 2 s to 4 s, decreases from 4 s to 6 s, decreases from 6 s to 8 s after the Mechanical control, and increases from 8 s to 10 s. The overall response fluctuates around -5 m/s^2, and the trend of change is relatively smooth. After the implementation of Mechanical control, the vibration of the bridge is smoother and the vibration response of the bridge is reduced.

(5) The dynamics of other vehicle-axle coupling systems, such as wheel-rail forces, are also significantly improved, which can effectively improve the stability and safety of the bridge vibration when the vehicle passes through.

Funding

This article requires the addition of a project support, with the following project information: The research described in this paper was financially supported by the Science and Technology Research Project of Henan Provincial Science and Technology Department(Grant No. 232102241008).

References

[1] Zhang, J.P., Li, X.P., Zhou, F.L. Development and Problems of Vibration Control of Bridge Structures. World Earthquake Engineering, 1998, 14(2):9–16.

[2] Zhou Fulin, Seismic Control of Engineering Structures. Beijing: Earthquake Press, 1997.

[3] Yao J. Concept of Structural Control. ASCE Journal of the Structural Division, 1972, 98(7):1567–1574.

[4] Truong QT, Phan DH. Numerical study of aeroelastic suppression using active control surfaces on a full-span suspension bridge. Structures, 2021, 33(1): 606–614.
[5] Phan D H. Aeroelastic control of bridge using active control surfaces an analytical and experimental study. Structures, 2020, 27: 2309–2318.
[6] Sangalli LA, Braun AL. A fluid-structure interaction model for numerical simulation of bridge flutter using sectional models with active control devices. Preliminary results. Journal of Sound and Vibration, 2020, 477: 115338.
[7] Bera KK, Chandiramani N K. Controlling flutter of a cable-stayed bridge with output feedback has driven winglets. Journal of Wind Engineering and Industrial Aerodynamics, 2020, 206(12):104372.
[8] Soares R W, Barroso L R, Al-Fahdawi O. Simple adaptive control to attenuate bridge's seismic responses considering parametric variations. advances In Structural Engineering, 2020, 23(1):132–145.
[9] Mei C. Hybrid wave/mode active control of bending vibrations in beams based on the advanced Timoshenko theory[J]. 322(1–2):29–38.
[10] Jung HJ, DD Jang, Choi K M, et al. Vibration mitigation of highway isolated bridge using MR damper-based smart passive control system employing an electromagnetic induction part. Structural Control & Health Monitoring, 2010, 16(6):613–625.
[11] Rosario Ceravolo, Nicola Tondini, Giuseppe Abbiati and Anil Kumar. dynamic characterization of complex bridge structures with passive control systems. Structural Control & Health Monitoring, 2012, 19(4): 511–534.
[12] Martinez-Rodrigo, M.D, Filiatrault A. A case study on the application of passive control and seismic isolation techniques to cable-stayed bridges: A comparative investigation through non-linear dynamic analyses. Engineering Structures, 2015, 99: 232–252.
[13] Soneji B B, Jangid R S. Passive hybrid systems for earthquake protection of cable-stayed bridge. engineering Structures, 2007, 29(1): 57–70.
[14] Wilde K, Fujino Y, Kawakami T. Analytical and experimental study on passive aerodynamic control of flutter of a bridge deck. journal of Wind Engineering & Industrial Aerodynamics, 1999, 80(1–2): 105–119.
[15] Mgs A, H B. Semi-active vibration control of smart isolated highway bridge structures using replicator dynamics. engineering Structures, 2019, 186. 536–552.

[16] Hormozabad S J, Soto M G. Load balancing and neural dynamic model to optimize replicator dynamics controllers for vibration reduction of highway bridge structures. engineering Applications of Artificial Intelligence, 2021, 99: 104138.
[17] Heo G, Seo S, Jeon S, et al. Development of a hybrid control algorithm for effective reduction of drift in multi-span isolated bridges. Soil Dynamics and Earthquake Engineering, 2021, 143(3):106659.
[18] Yang Tailai, Simulation and Experimental Research on Adaptive Bearing Control Technology of Elevated Floating Bridge for Deep Water Railway Bridge Repair. Shijiazhuang: Shijiazhuang Railway University, 2021.
[19] Hu Hongsheng, Research on Active Control of Vibration of Moving Mass Excited Beams. Nanjing: Nanjing University of Science and Technology, 2005.
[20] Qiu, C.C., Chen, S.W., Active control of vibration in a mobile flexible beam system. Vibration, Testing and Diagnostics, 2022, 42(1): 62–67+194.
[21] Zx A, Bh B, Hz B, et al. Extemal suction-blowing method for controlling vortex-induced vibration of a bridge[J]. Industrial Aerodynamics, 2021, 215: 104661.
[22] Li W, Yang Z, Li K, et al. Hybrid feedback PID-FxLMS algorithm for active vibration control of cantilever beam with piezoelectric stack actuator. Journal of Sound and Vibration, 2021, 509: 116243.
[23] Xiong Chunhui. Structural vibration passive control of large-span cable-stayed bridge based on fluid dampers. Wuhan: Wuhan University of Technology, 2011.
[24] Zhang Mingxiang. Research on wind-induced vibration analysis and passive control of large-span bridges. Hefei: Hefei University of Technology, 2011.
[25] Liu Chengbin, Huang Hongbo, Wang Baisheng. Application of TMD on bridge vibration control and its theoretical analysis, Municipal Technology, 2003(3):137–139.
[26] Wang Taiheng et al. Analysis of Factors Influencing Mechanical Properties of Corrugated Steel Based on Entropy Method. European Journal of Computational Mechanics, 2022, 31(4): 539–554.
[27] Li Rui, Zhou Mengjiao, Wu Mengjuan, et al Semi-Active Predictive Control of Isolated Bridge Based on Magnetorheological Elastomer Bearing. University, 2019, 24(1):64–70.

[28] Li Xue-You, Zhang Yin. Semi-active control test of multi-modal vibration of the inclined cable. Journal of Civil Engineering and Management, 2021, 38(1): 100–105.
[29] J.G. Walker, N.S. Ferguson, M.G. Smith. An investigation of noise from trains on bridges. Journal of Sound and Vibration, 1996, 193(1): 307–314.
[30] Jean P. A variational approach for the study of outdoor sound propagation and application to railway noise. Journal of sound and vibration, 1998, 212(2): 275–294.

Biographies

Ma Zhifang received her master's degree in engineering from Dalian University of Technology in 2013. Currently, she serves as a lecturer in the School of Railway Engineering, Zhengzhou Railway Vocational and Technical College. Her research field mainly covers bridge engineering.

Sun Zhuoyu obtained a Bachelor's degree in Bridge and River Crossing Engineering from Tianjin Urban Construction in 2015, followed by a Master's degree in Road and Railway Engineering from Dalian Jiaotong

University. He is currently a teacher at the School of Railway Engineering at Zhengzhou Railway Vocational and Technical College, mainly focusing on earthquake prevention and disaster reduction in tunnel engineering.

Yuan Yuan received her master's degree in engineering from Zhengzhou University in 2016. Currently, she serves as a professor in the School of Railway Engineering, Zhengzhou Railway Vocational and Technical College. Her research field mainly covers structural engineering.